

A MPC Walking Framework With External Contact Forces

Sean Mason¹, Nicholas Rotella¹, Stefan Schaal^{1,2}, and Ludovic Righetti^{2,3}

Abstract—In this work, we present an extension to a linear Model Predictive Control (MPC) scheme that plans external contact forces for the robot when given multiple contact locations and their corresponding friction cone. To accomplish this we set up a two step optimization problem. In the first optimization, we compute the Center of Mass (CoM) trajectory, foot step locations, and introduce slack variables to account for violating the imposed constraints on the Center of Pressure (CoP). We then use the slack variables to trigger the second optimization, in which we calculate the optimal external force that compensates for the CoP tracking error. This optimization considers multiple contacts with the environment by formulating the problem as a Mixed Integer Quadratic Program (MIQP) that can be solved at the order of 100 Hz. Once contact is created, the MIQP collapses to a single Quadratic Program (QP) that can be solved in real time < 1kHz. Simulations show that the presented control scheme can withstand disturbances 2-5x larger with the additional force provide by a hand contact when considering delays and 3-6x larger when contact is already made.

I. INTRODUCTION

In bipedal locomotion, online pattern generators have seen much success because of their ability to adapt to the continually changing environment and internal states. In order to generate new plans quickly, researchers typically utilize a simplified dynamic model for fast planning of center of mass (CoM) trajectories. The plans are then tracked using a whole-body controller typically utilizing either inverse kinematics or inverse dynamics. The Linear Inverted Pendulum Model (LIPM) the most important model for biped walking because it is linear and yet effectively captures the dynamics for walking on flat surfaces. Because the LIPM is low dimensional and linear, its dynamics can be regulated through linear control methods for compact formulations and efficient computations.

In [1], Kajita et. al introduced the preview control of the LIPM which optimizes the CoM trajectory over a horizon. For a linear system with no inequality constraints, this is equivalent to solving the well known finite horizon Linear Quadratic Regulator (LQR) which additionally yields a time varying feed-forward and feedback policy. If the system

includes inequality constraints, the solution no longer provides a feedback policy to stabilize the trajectory. To rectify this, Model Predictive Control (MPC) is used. Feedback is then generated by continuously resolving the constrained optimization from the measured state and applying the first feedforward command. In [2], Center of Pressure (CoP) constraints in the form of linear inequalities are introduced and the problem is solved in a receding horizon to produce CoM trajectories robust to perturbations. This approach was further extended in [3] to additionally optimize over the footstep locations, allowing the robot to take recovery steps. Researchers have further developed MPC methods using the LIPM to adjust footstep timing [4], [5], [6], to plan 3D trajectories [7], to control the Divergent Component of Motion (DCM) [8], [9] and a nonlinear extension allowed to deal with obstacles [10].

The problem of designing receding horizon controllers that handle rough terrain and allow the use of hand contacts largely remain open. More general model such as the centroidal momentum dynamics have gained popularity to generate patterns allowing multi-contact behaviors [11], [12] but they are not convex and are computationally more demanding. While significant progress has been made with these algorithms, they have to date not been applied for receding horizon control of legged robots.

Simpler models still allowing hand contacts have also been explored. In [13], hand contacts with the environment were introduced in a MPC problem by deriving a non-linear dynamical model of the CoM that included an external wrench. To solve the non-linear optimization problem a Newton scheme was presented in which each step of the optimization was bounded such that the intermediate solutions were always feasible. While external contacts were used for stability, footstep and contact locations and timing were pre-determined. Additionally, the contact considered was a grasp and not a push, thus neglecting friction cone constraints. In [14], an external wrench is also included in the MPC scheme to design a walking pattern generator for physical collaboration. To drive cooperation with a second agent, the robot assumes the role of either a leader or follower in the task of collectively carrying an object. Contact forces are included in the dynamics and cost function in such that the problem remains linear in the constraints and quadratic in the cost.

In this paper, we are interested in extending pattern generators based on the LIPM model to allow the use of hand contacts when stability cannot be maintained by stepping only. Our approach keeps computational complexity low to allow receding horizon control. Our idea is to treat the hand

This research was supported in part by National Science Foundation grants IIS-1205249, IIS-1017134, EECs-0926052, the Office of Naval Research, the Okawa Foundation, and the Max-Planck-Society. Any opinions, findings, and conclusions or recommendations expressed in this material are those of the author(s) and do not necessarily reflect the views of the funding organizations.

¹Computational Learning and Motor Control Lab, University of Southern California, Los Angeles, California.

²Autonomous Motion Department, Max Planck Institute for Intelligent Systems, Tuebingen, Germany.

³Tandon School of Engineering, New York University, New York, USA

contact has a complement to the feet motions. Our approach then proposes a two-part optimization approach that automatically calculates how to use the hand supports when the CoM and footstep adjustment alone is not sufficient. The contact locations are chosen among multiple contact points, time to contact is optimized and it considers friction cone constraints. Our decomposition keeps the computational simplicity of preview controllers based on the LIPM dynamics in the first optimization. The second part then selects a hand contact location and contact force to stabilize the robot when necessary by solving a low dimensional mixed integer quadratic program. The result is a controller that reactively decides to use the robot hands to stabilize walking only when necessary. Push recovery simulation experiments demonstrate that our approach can significantly improve the stability of a walking robot under strong perturbations.

The paper is organized as follows. Section II begins by deriving the CoM dynamics from the Newton-Euler equations for the LIPM with the addition of an external contact force. Section IV explains the 2-step optimization scheme to compute trajectories for the CoM, footstep locations, and external contact force. Section V presents an evaluation of the control scheme using a simplified upper body representation and a fully articulated torque controller lower body controlled through inverse dynamics.

II. NEWTON-EULER DYNAMICS

Similar to [14] we separate foot contact forces, f_i , from all other forces in the Newton-Euler Equations (1), (2). We define the hand contact force as f_c which is located at point p .

$$m(\ddot{c} + g) = f_c + \sum f_i \quad (1)$$

$$c \times m(\ddot{c} + g) + \dot{L} = p \times f_c + \sum s_i \times f_i \quad (2)$$

In these equations, c is the CoM, L is the angular momentum and s_i is the location of the co-planar foot contacts. Dividing the Euler equation by the Z term of the Newton equation and rearranging yields

$$\frac{\sum s_i \times f_i}{\sum f_i^z} = \frac{c \times m(\ddot{c} + g) - (p \times f_c) + \dot{L}}{m(\ddot{c}^z + g) - f_c^z}.$$

Under the LIPM assumptions, the angular momentum is constant ($\dot{L} = 0$), and the CoM height is constant ($\ddot{c}^z = 0$), with the ground plan at 0 ($s_i^z = 0$). We can then write the equations for the Zero Moment Point (ZMP) which we will refer to as Z_{hand} (ZMP with external hand contact)

$$Z_{\text{hand}}^{x,y} = \frac{\sum s_i^{x,y} f_i^z}{\sum f_i^z} = -\frac{mc^z \ddot{c}^{x,y} - mgc^{x,y} - p^z f_c^{x,y} + p^{x,y} f_c^z}{mg - f_c^z} \quad (3)$$

We notice that the external contact force multiplies the contact point and that if there is no contact force, i.e. $f_c = 0$, this term reduces to the familiar ZMP equations for the LIPM, Z_{lipm}

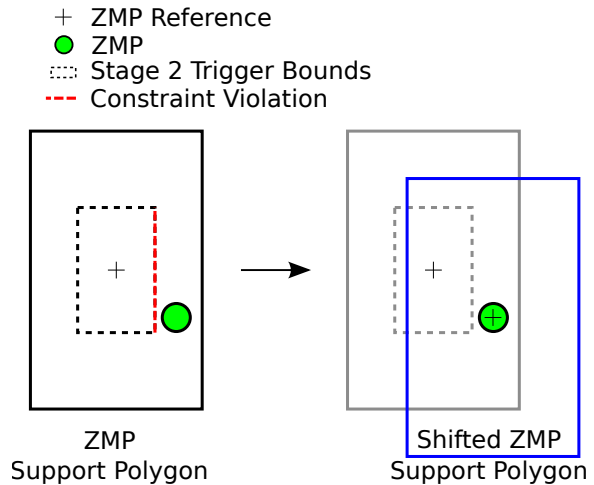


Fig. 1. When the conservative ZMP bounds are violated the robot seeks to create a contact force among the available options such that the "Shifted ZMP Support Polygon", Eq. (7) is centered at the current ZMP location.

$$Z_{\text{lipm}}^{x,y} = \frac{\sum s_i^{x,y} f_i^z}{\sum f_i^z} = c^{x,y} - \frac{c^z \ddot{c}^{x,y}}{g} \quad (4)$$

III. DECOMPOSITION OF THE ZMP

To express the relationship between the LIPM with and without a hand contact, we can write the full ZMP expression in terms of the ZMP without external forces as

$$Z_{\text{hand}} = Z_{\text{lipm}} + \Delta Z \quad (5)$$

By expressing the ZMP this way we can think about how the ZMP changes with the addition of an external force. As mentioned in [14], we can additionally think about the implication of this force on the ZMP bounds. That is, we can rewrite

$$Z \leq Z_{\text{lipm}} + \Delta Z \leq \bar{Z} \quad (6)$$

as

$$Z - \Delta Z \leq Z_{\text{lipm}} \leq \bar{Z} - \Delta Z. \quad (7)$$

One way to think about this, is that we shift the support polygon for the ZMP corresponding to the original LIPM through the addition of an external force. Solving for ΔZ yields

$$\Delta Z^{x,y} = \left(\frac{p^z}{mg - f_c^z} \right) f_c^{x,y} + \left(\frac{-p^{x,y} - \frac{c^z \ddot{c}^{x,y}}{g} + c^{x,y}}{mg - f_c^z} \right) f_c^z \quad (8)$$

which expresses how the addition of a hand contact is equivalent to increasing the ZMP support area.

IV. OPTIMIZATION FORMULATION

In order to calculate the contact force and locations for the robot's hand we propose a two part optimization in which the hand contact is planned to compensate for the ZMP constraint violations. The result is a walking controller that

re-actively uses hand contacts when the control of the CoM and footstep locations alone is insufficient. An outline of the algorithm is shown below.

```

while Robot Has Not Fallen do
  Find reachable contact points from list.
  Constrain slack variables based on time to reach
  contact
  Solve LIPM based MPC (Sec. #) to generate
  CoM, footstep, and slack trajectory.
  if  $\|Slack\ Trajectory\| > 0$  then
    if Hand In Contact then
      Solve QP to calculate the external force that
      compensates for the ZMP error (Sec. #)
    else
      Solve MIQP to decide the best contact
      location (Sec #).
      Track solution with hand.
    end
  end
end

```

Algorithm 1: MPC Walking Scheme With Hand Contacts

A. Stage 1: MPC of CoM Trajectory and Footstep Locations

In the first stage of the optimization, we formulate a MPC scheme to minimize CoM jerk, ZMP tracking error, and CoM velocity tracking error and solve as a QP. The scheme is based on the well known approach from [3] so we omit the details of model for brevity. The only difference in the approach is that we write the ZMP constraints with the addition of a trajectory of slack variables, $S_k, k = 1 \dots N$, where N is the length of the preview horizon in the MPC. We can write this constraint in the same form as Eq. (7), omitting the subscript k , as

$$\underline{Z} - S \leq Z_{lipm} \leq \bar{Z} - S, \quad (9)$$

where \underline{Z} and \bar{Z} correspond to a shrunken support polygon. The amount we shrink the support polygon is directly linked to how early the hand contact will be triggered to help, refer to Fig. 1. When $|S| > 0$, it means that extra support from another contact is necessary to maintain balance and this triggers the use of a hand contact. In order to account for the fact that it will take some time for the hand to reach the contact point location, we constrain the first N_D time steps of the horizon to be zero, where $N_D = (\text{distance}/V)/dt$. Furthermore, we add a weighted quadratic term to minimize the S in the QP cost function to favor solutions that only use feet for balance.

B. Stage 2: Hand Contact

This section outlines the major contribution of this paper. Once the first optimization signifies the need for assistance of a hand contact (i.e. $|S| > 0$), a second optimization stage calculates the necessary contact force to shift the ZMP boundaries such that the current ZMP matches the reference. When the hand has not yet created a contact, we formulate a

MIQP that includes all the reachable contact point locations along with their corresponding friction cones to determine which, if any, is the optimal contact location to counteract for the ΔZ trajectory, where $\Delta Z = Z_{lipm} - Z_{ref}$. Once a contact has been made, we remove all other contacts from the optimization and solve a QP at each time step (1kHz) to determine the contact force. We begin by formulating the problem for when the hand is already in contact.

C. Determining the Contact Force

In Eq. (8), we can see that with the values of $\Delta Z^{x,y}$ determined, we have two equations and three unknowns. Geometrically, the solutions for the 3D force vector from a line that can be rewrite in parametric form as

$$\mathbf{f}_c^{x,y} = \frac{p^{x,y} + \frac{c^z \ddot{c}^{x,y}}{g} - c^{x,y} - \Delta Z^{x,y}}{p^z} \mathbf{f}_c^z + \frac{mg \Delta Z^{x,y}}{p^z} \quad (10)$$

Note that $\mathbf{f}_c^{x,y}$ is a linear function of \mathbf{f}_c^z and thus the only decision variable in the QP is \mathbf{f}_c^z . We include friction cone constraints by first changing the frame of our variables to be aligned with the surface normal of the contact.

$$\begin{bmatrix} f^b \\ f^t \\ f^n \end{bmatrix} = R \begin{bmatrix} f^x \\ f^y \\ f^z \end{bmatrix} \quad (11)$$

and write the following constraints

$$f^b \leq u f^n \quad f^b \geq -\mu f^n \quad (12)$$

$$f^t \leq u f^n \quad f^t \geq -\mu f^n \quad (13)$$

$$f^n \leq f_{max}^n \quad f^n \geq 0, \quad (14)$$

where μ is the static coefficient of friction that defines the friction cone. The cost function to optimize is then

$$\text{minimize}_{\mathbf{f}_c^z} \quad (f^b)^2 + (f^t)^2 + \kappa (f^n)^2$$

subject to Friction Cone Constraints

The gain κ allows one to prioritize solutions that are closer to the center of the friction cone and thus more robust to slipping. Because the formulation shown in this section compensates exactly for the ΔZ measured from the system, the optimization does not consider the bounds of the original support polygon, refer back to Fig. 1. It is possible that there is no feasible \mathbf{f}_c that exactly compensates for ΔZ , but there does exist a \mathbf{f}_c that moves the ZMP inside the "shifted ZMP support polygon". To address this, we can include a new slack variable S_z .

$$\underline{Z} \leq \Delta Z + S_z \leq \bar{Z} \quad (15)$$

Note that in this expression ΔZ is already defined. Rewriting this as a function of S_z and \mathbf{f}_z give us

$$\mathbf{f}_c^{x,y} = \frac{p^{x,y} + \frac{c^z \ddot{c}^{x,y}}{g} - c^{x,y} - (\Delta Z^{x,y} + S_z^{x,y})}{p^z} \mathbf{f}_c^z + \frac{mg(\Delta Z^{x,y} + S_z^{x,y})}{p^z}$$

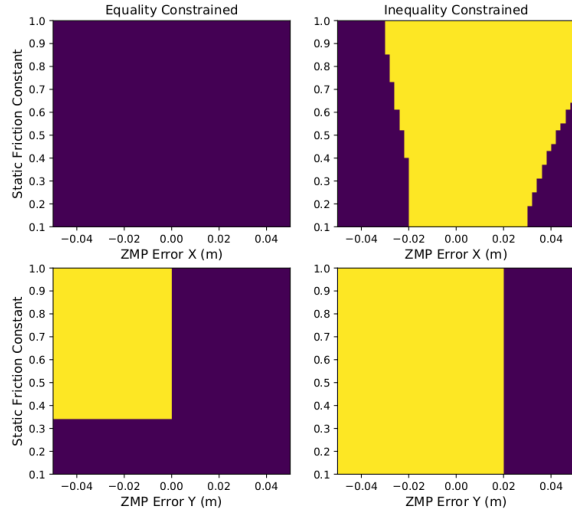


Fig. 2. An example in which we sweep over different parameters for the friction coefficient and ZMP tracking error and plot whether the problem formulation found an optimal solution. Yellow means a solution was found and blue means the optimization failed. In this example the following parameters were used. $c = [0.0, 0.0, .6]$, $\tilde{c} = [0.0, 0., 0.0]$, $p = [.2, 0, 1]$, $m = 52$, $R = \text{rot}([-90, -20, 10])$ where $\text{rot}()$ is a rotations matrix formed from angles in the x-y-z sequence. This plot simply demonstrates the expanded ability to find optimal solutions by using the inequality form of the problem, Eq. (15)

$$\mathbf{f}_c^{x,y} = \frac{p^{x,y} + \frac{c^z \tilde{c}^{x,y}}{g} - c^{x,y} - \Delta Z^{x,y}}{p^z} \mathbf{f}_c^z + \frac{1}{p^z} \mathbf{S}_z^{x,y} \mathbf{f}_c^z + \frac{mg}{p^z} \mathbf{S}_z^{x,y} + \frac{mg \Delta Z^{x,y}}{p^z}.$$

By doing this, we introduce a new decision variables $\mathbf{S}_z^{x,y}$ and create the bilinear term $\mathbf{S}_z^{x,y} \mathbf{f}_c^z$. To address this, we introduce a new variable \mathbf{W} and relax the constraint $\mathbf{W} = \mathbf{S}_z^{x,y} \mathbf{f}_c^z$ by including a McCormick envelope[15].

As shown in Fig. 2, by solving for contact forces using this formulation we expand the region for which the QP solver finds solutions.

D. Determining the Contact Location

In order to determine the contact location, we reason about reachable contact locations and their corresponding friction cone in the form of a MIQP. To define whether a contact has been chosen, we introduce the binary variables $b_i \in \{0, 1\}$, $i = 1 \dots N_c$. We define a reachability sphere as $\|c_k - p_k\| < r$, where r is the radius. We then optimize over the time steps \hat{k} in the slack trajectory defined $|S_k| > 0$ ($\hat{k} = k[|S_k| > 0]$).

$$\begin{aligned} & \underset{f_i^z \hat{k}, b_i}{\text{minimize}} && (f^b)_{i\hat{k}}^2 + (f^t)_{i\hat{k}}^2 + \kappa (f^n)_{i\hat{k}}^2 \\ & \text{subject to} && \end{aligned}$$

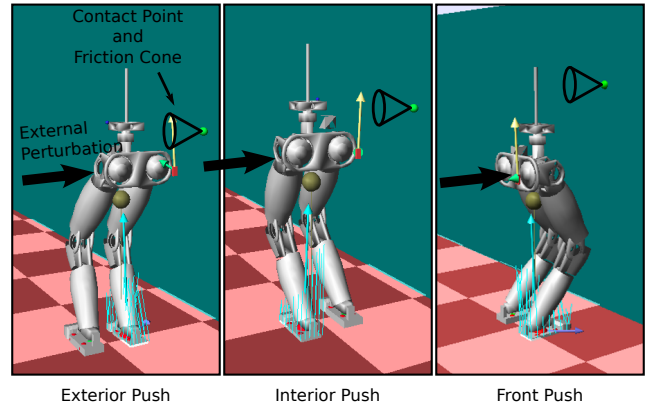


Fig. 3. Configurations used for the push recovery experiments. The exterior and interior push differ by which foot is in single support at the time of the push.

$$\sum_1^{N_c} b_i = 1 \quad (16)$$

$$b_i \implies \begin{cases} 0, & f_{i\hat{k}}^z = 0 \\ 1, & (\text{Friction Cone Constraints})_i \end{cases} \quad (17)$$

V. EXPERIMENTS

In this section, we evaluate the proposed control scheme through a series of push recovery tests while the robot is walking. We use a dynamic simulation of a humanoid robot with a simplified upper body; the effect of an external hand contact with the environment is transformed to the torso of the robot and applied as a wrench. In order to account for the time it would take the humanoid to move its hand to the contact point, we add a lower bound on the time which must elapse before the contact is simulated.

The plots in 4 show the results from experiments in which we push the robot towards a wall with a known contact point. The robot is pushed to the exterior, interior, and front with a wall located in the direction of push. We plot the external force applied, the resulting contact force calculated from the controller, the CoM motion, and the ZMP tracking. For each of these experiments, the following common parameters were used:

Mass	52 kg
CoM Height	.62m
Single Support	1.0 s
Double Support	0.1 s
ZMP Bounds Scaling Factor	.1
MPC Horizon	1.6 s
MPC dt	.1 s
Max Normal Force	100 N
μ	1
Contact Height	1.1 m

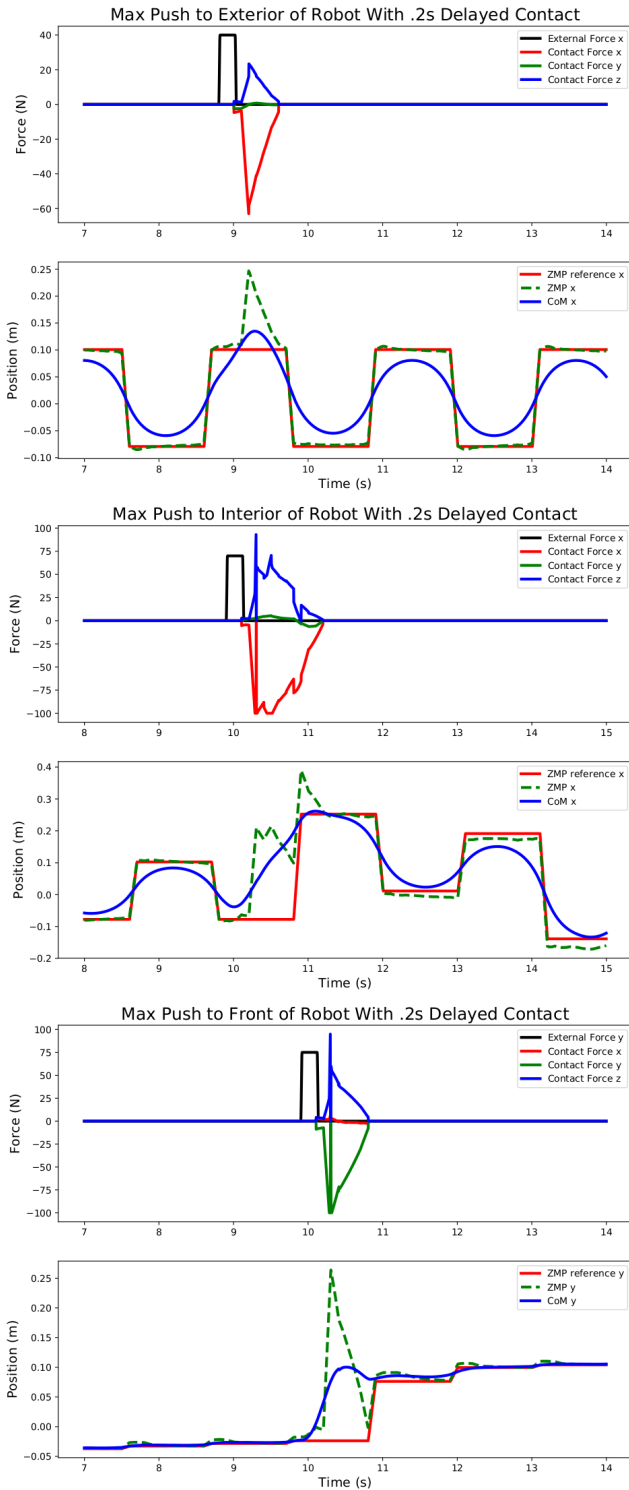


Fig. 4. Push recovery results for the three scenarios shown in Fig. 3. These tests were all conducted when the robot was originally walking in place with a time delay of 0.2 s. The reference ZMP indicates where the current stance foot is located.

The scenarios presented in 4 represent three canonical push recovery situations. The exterior push show a situation in which the disturbance cannot be compensated by adjusting

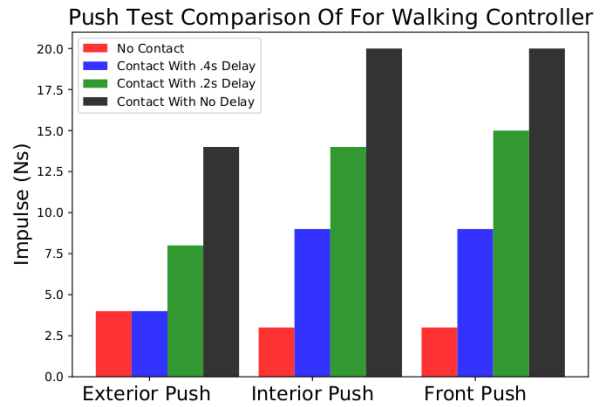


Fig. 5. Side-by-side comparison of the max impulse for the walking controller with and without the use of an external contact.

the footstep plan alone (unless footstep crossover would be allowed). The ability for the robot to produce a reactive hand contact force is important in situations in which the necessary recovery steps are not feasible. The interior push highlights a situation where both footstep plan adjustments and hand contacts are used to recover from an impulse of over 4.6 times the magnitude of the maximum baseline push. Finally, the front push shows a recovery in a direction orthogonal to the previous tests. In this situation, both footstep plan adjustments and hand contacts are again used to recover from the largest impulse tested in this set of experiments (15 Ns).

In order to investigate how varying amounts of delay between the disturbance and created contact times affect controller performance, we experimentally determined the maximum impulse for instantaneous contact, a 0.2 second delay, a 0.4 second delay, and for no contact at all. As expected, Fig. 5 shows the diminishing ability of the control scheme to recover as the magnitude of delay increases. This emphasizes the importance of quick reaction time in compensating for unexpected disturbances. In order to track the CoM and footstep trajectory we use an optimization-based whole-body inverse dynamics controller, similar to [16], [17], [18], [19], to resolve for joint torques at 1kHz. Further demonstrations of the behavior of this control scheme are shown in the accompanying video.

VI. CONCLUSION

In this work, we presented an extension to an MPC walking control scheme that plans reactively plans which contact to use and what force to create. In doing so, the formulation consider friction properties of the contact surfaces and also the time it takes to move your hand to to contact location. To accomplish this, we introduced a 2 stage optimization scheme in which the first optimization plans the CoM and footsteps trajectories while the second optimization reasons about the hand contacts. The second optimization is initiated when the first optimization violates some conservative ZMP constraints. We found that formulations that combined these two optimization steps, as we have presented them, were

much to slow to provide a reactive feedback. As shown in our experiments, the benefit of using hand contact together with a walking controller similar to the one presented decreases significantly when large delays are introduced. Additionally, because this control scheme separates walking from hand contacts there is the possibility to pair the second stage with different LIPM based walking pattern generators and invites other methods it trigger the need for hand contact. Potential directions for future research would be to use the DCM of the LIPM or to an external force estimator [20] to trigger the need for hand contact. Future experiments will focus on incorporating the upper body in the inverse dynamics solver and validating the control scheme in more complicated environments gauge the practicality of this control scheme for use on a real robot.

REFERENCES

- [1] S. Kajita, F. Kanehiro, K. Kaneko, K. Fujiwara, K. Harada, K. Yokoi, and H. Hirukawa, "Biped walking pattern generation by using preview control of zero-moment point," *2003 IEEE International Conference on Robotics and Automation (Cat. No.03CH37422)*, pp. 1620–1626, 2003. [Online]. Available: <http://ieeexplore.ieee.org/lpdocs/epic03/wrapper.htm?arnumber=1241826>
- [2] P.-b. Wieber, "Trajectory Free Linear Model Predictive Control for Stable Walking in the Presence of Strong Perturbations," *2006 6th IEEE-RAS International Conference on Humanoid Robots*, pp. 137–142, dec 2006. [Online]. Available: <http://ieeexplore.ieee.org/lpdocs/epic03/wrapper.htm?arnumber=4115592>
- [3] A. Herdt, H. Diedam, P. brice Wieber, D. Dimitrov, K. Mombaur, and M. Diehl, "Online walking motion generation with automatic foot step placement," in *Online*. Available: <https://groups.csail.mit.edu/robotics-center/elib/papers/Herdt10.pdf>, 2010, pp. 5–6.
- [4] M. Khadiv, A. Herzog, S. A. a. Moosavian, and L. Righetti, "Step Timing Adjustment : A Step toward Generating Robust Gaits *," 2016.
- [5] M. R. O. A. Maximo, C. H. C. Ribeiro, and R. J. M. Afonso, "Mixed-Integer Programming for Automatic Walking Step Duration," no. 3, pp. 5399–5404, 2016.
- [6] S. Caron and Q.-C. Pham, "When to make a step? Tackling the timing problem in multi-contact locomotion by TOPP-MPC," no. 1, 2016. [Online]. Available: <http://arxiv.org/abs/1609.04600>
- [7] C. Brasseur, A. Sherikov, C. Collette, D. Dimitrov, and P. B. Wieber, "A robust linear MPC approach to online generation of 3D biped walking motion," *IEEE-RAS International Conference on Humanoid Robots*, vol. 2015-Deceem, pp. 595–601, 2015.
- [8] J. Engelsberger, T. Koolen, S. Bertrand, J. Pratt, C. Ott, and A. Albu-Sch?ffer, "Trajectory generation for continuous leg forces during double support and heel-to-toe shift based on divergent component of motion," *IEEE International Conference on Intelligent Robots and Systems*, no. Iros, pp. 4022–4029, 2014.
- [9] M. A. Hopkins, D. W. Hong, and A. Leonessa, "Humanoid locomotion on uneven terrain using the time-varying divergent component of motion," *IEEE-RAS International Conference on Humanoid Robots*, vol. 2015-Febru, pp. 266–272, 2015.
- [10] M. Naveau, M. Kudruss, O. Stasse, C. Kirches, K. Mombaur, and P. Souères, "A reactive walking pattern generator based on nonlinear model predictive control," *IEEE Robotics and Automation Letters*, vol. 2, no. 1, pp. 10–17, Jan 2017.
- [11] J. Carpentier, S. Tonneau, M. Naveau, O. Stasse, and N. Mansard, "A versatile and efficient pattern generator for generalized legged locomotion," in *ICRA*, 2016.
- [12] A. Herzog, S. Schaal, and L. Righetti, "Structured contact force optimization for kino-dynamic motion generation," *IROS*, 2016. [Online]. Available: <http://arxiv.org/abs/1605.08571>
- [13] D. Serra, C. Brasseur, A. Sherikov, D. Dimitrov, and P. B. Wieber, "A newton method with always feasible iterates for nonlinear model predictive control of walking in a multi-contact situation," in *2016 IEEE-RAS 16th International Conference on Humanoid Robots (Humanoids)*, Nov 2016, pp. 932–937.
- [14] D. J. Agravante, A. Sherikov, P. B. Wieber, A. Cherubini, and A. Kheddar, "Walking pattern generators designed for physical collaboration," in *2016 IEEE International Conference on Robotics and Automation (ICRA)*, May 2016, pp. 1573–1578.
- [15] P. Castro and F. de Cincias, "Tightening piecewise mccormick relaxations through partition-dependent bounds for non-partitioned variables," 11 2014.
- [16] S. Feng, E. Whitman, X. Xinjilefu, and C. G. Atkeson, "Optimization based full body control for the atlas robot," *IEEE-RAS International Conference on Humanoid Robots*, vol. 2015-February, no. Id, pp. 120–127, 2015.
- [17] A. Herzog, N. Rotella, S. Mason, F. Grimminger, S. Schaal, and L. Righetti, "Momentum control with hierarchical inverse dynamics on a torque-controlled humanoid," *Autonomous Robots*, vol. 40, no. 3, pp. 473–491, Mar. 2016.
- [18] R. Tedrake *et al.*, "A summary of team mit's approach to the virtual robotics challenge," in *Robotics and Automation (ICRA), 2014 IEEE International Conference on*, May 2014, pp. 2087–2087.
- [19] T. Koolen *et al.*, "Summary of team ihmc's virtual robotics challenge entry," in *Humanoid Robots (Humanoids), 2013 13th IEEE-RAS International Conference on*, Oct 2013, pp. 307–314.
- [20] N. Rotella, A. Herzog, S. Schaal, and L. Righetti, "Humanoid momentum estimation using sensed contact wrenches," in *2015 IEEE-RAS 15th International Conference on Humanoid Robots (Humanoids)*, Nov 2015, pp. 556–563.